THE JOURNAL OF BIOLOGICAL CHEMISTRY
Vol. 277, No. 32, Issue of August 9, pp. 29224–29230, 2002

Printed in U.S.A.

Ion Permeation of AQP6 Water Channel Protein

SINGLE-CHANNEL RECORDINGS AFTER Hg^{2+} ACTIVATION*

Received for publication, May 1, 2002, and in revised form, May 21, 2002
Published, JBC Papers in Press, May 28, 2002, DOI 10.1074/jbc.M204258200

Akihiro Hazama‡, David Kozono¶, William B. Guggino‖, Peter Agre¶, and Masato Yasui§¶‡‡**

*From the ‡Okazaki National Research Institutes, Center for Integrative Bioscience, Okazaki, 444-8585, Japan and the Departments of ¶Biological Chemistry, ‖Physiology, **Medicine, and ‡‡Pediatrics, Johns Hopkins University School of Medicine, Baltimore, Maryland 21205*

Aquaporin-6 (AQP6) has recently been identified as an intracellular vesicle water channel with anion permeability that is activated by low pH or $HgCl_2$. Here we present direct evidence of AQP6 channel gating using patch clamp techniques. Cell-attached patch recordings of AQP6 expressed in *Xenopus laevis* oocytes indicated that AQP6 is a gated channel with intermediate conductance (49 picosiemens in 100 mM NaCl) induced by 10 μM $HgCl_2$. Current-voltage relationships were linear, and open probability was fairly constant at any given voltage, indicating that Hg^{2+}-induced AQP6 conductance is voltage-independent. The excised outside-out patch recording revealed rapid activation of AQP6 channels immediately after application of 10 μM $HgCl_2$. Reduction of both Na^+ and Cl^- concentrations from 100 to 30 mM did not shift the reversal potential of the Hg^{2+}-induced AQP6 current, suggesting that Na^+ is as permeable as Cl^-. The Na^+ permeability of Hg^{2+}-induced AQP6 current was further demonstrated by $^{22}Na^+$ influx measurements. Site-directed mutagenesis identified Cys-155 and Cys-190 residues as the sites of Hg^{2+} activation both for water permeability and ion conductance. The Hill coefficient from the concentration-response curve for Hg^{2+}-induced conductance was 1.1 ± 0.3. These data provide the first evidence of AQP6 channel gating at a single-channel level and suggest that each monomer contains the pore region for ions based on the number of Hg^{2+}-binding sites and the kinetics of Hg^{2+}-activation of the channel.

Aquaporins are a family of membrane channel proteins that are selectively permeated by water molecules (1). Ion permeability is not a general feature of aquaporins (2, 3); however, we recently demonstrated ion permeation via AQP6[1] expressed in *X. laevis* oocytes in response to Hg^{2+} or low pH (4). This unique characteristic of AQP6 may expand our understanding of biophysical aspects of aquaporins. Channel gating is a fundamental property of ion channels in response to certain stimuli, such as membrane potential, pH, or ligands. In contrast, evidence of rapid channel gating has never been directly demonstrated for any aquaporin. This may be because aquaporins are constitutively active rather than gated or because of technical limitations in the measurement of single-channel water conductance. Ion permeation through AQP6 at a single-channel level allows us to study whether this aquaporin is gated.

Mercurials are known to react with free sulfhydryls and to inhibit the osmotic water permeability of aquaporins (5). Site-directed mutagenesis identified the residue Cys-189 as the site of mercurial inhibition of AQP1 (6). Atomic structures of AQP1 have revealed that Cys-189 is located at the narrowest constriction of the channel pore, which led us to conclude that binding of Hg^{2+} to Cys-189 may occlude the pore, thereby inhibiting water conductance (7–9). Interestingly, AQP6 has a cysteine residue (Cys-190) at the corresponding position to the Cys-189 in AQP1. Nevertheless Hg^{2+} does not inhibit AQP6 as initially reported (10) but activates AQP6 instead (4). This raises the possibility that the mechanistic effects of Hg^{2+} on aquaporins may be more complex than previously thought.

Although Hg^{2+} induces both osmotic water permeability and ion conductance in AQP6, it remains unclear whether water and ions share a common pathway. Recent advances in developing atomic-resolution structural models of AQP1 and the bacterial glycerol transporter, GlpF, allow us to study detailed structure-function relationships (11–14). Aquaporins are present in the membrane as a homotetramer. It was recently suggested that the 4-fold axis of symmetry at the center of the homotetramer is a potential ion channel, based on the crystal structure of GlpF (15). No experimental data have yet been demonstrated to support this hypothesis, however.

Here, we study single-channel properties of AQP6 expressed in *X. laevis* oocyte plasma membranes using patch clamp techniques to advance our understanding of the biophysical properties of AQP6. We have determined the single-channel conductance of AQP6. We also demonstrate the most likely ionic pathway for AQP6 based on the kinetics of Hg^{2+} activation of the channel.

MATERIALS AND METHODS

Oocyte Preparation and Expression—Stage V-VI oocytes were harvested from adult *X. laevis* anesthetized by immersion in ice-cold water. Ovarian follicles were removed, cut into small pieces, and digested in Ca^{2+}-free OR2 (100 mM NaCl, 1 mM $MgCl_2$, 2 mM KCl, and 5 mM HEPES, pH 7.5) solution containing 2 mg/ml collagenase type IA (Sigma) for 1–2 h at room temperature. The oocytes were extensively rinsed with OR2 solution without collagenase and placed in Modified Barth's solution (MBS) at 18 °C. The oocytes were injected the day after isolation with either 50 nl of water (control) or 50 nl of water containing 5 ng of wild-type or mutant rat AQP6 cRNA. Mutations were introduced into AQP6 using the Chameleon double strand, site-directed mutagenesis

* This work was supported by Grants-in-aid for Scientific Research 12670051 and 13027289 (to A. H.) from the Japanese Ministry of Education, Culture, Sports Science and Technology, Grants DK32753 (to W. B. G.) and HL33991, HL48268, and EY11239 (to P. A.) from the National Institutes of Health, a grant from the American Heart Association (to M. Y.), and a grant from Itoh Foundation U. S. A. (to M. Y.). The costs of publication of this article were defrayed in part by the payment of page charges. This article must therefore be hereby marked "*advertisement*" in accordance with 18 U.S.C. Section 1734 solely to indicate this fact.

§ To whom correspondence should be addressed: Dept. of Pediatrics and Biological Chemistry, Johns Hopkins University School of Medicine, 725 N. Wolfe St., Baltimore, MD 21205-2185. Tel.: 410-955-3154; Fax: 410-955-3149; E-mail: myasui@jhmi.edu.

[1] The abbreviations used are: AQP, aquaporin; I-V, current-voltage.

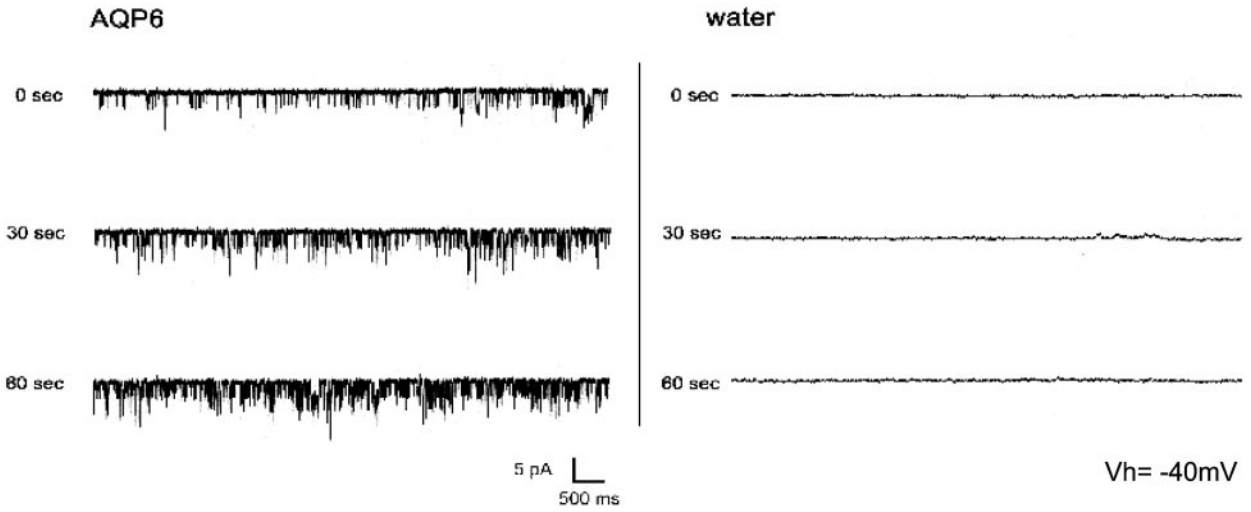

FIG. 1. **Cell-attached patch recording of an AQP6-expressing oocyte.** Representative current traces from the membrane of an AQP6 oocyte (*left panel*) and water-injected control oocyte (*right panel*) are shown ($n = 5$). The currents were measured at −40 mV. The electrode tip was dipped into Hg^{2+}-free standard pipette solution for 10 s, and then the pipette was backfilled with 30 μM $HgCl_2$-containing solution. The Hg^{2+} concentration at the tip of the pipette was expected to increase gradually during the experiment. The membrane potential was simply estimated as the inverse of the holding potential because the resting membrane potential of oocyte became almost zero during the manual removal of the vitelline membrane.

kit (Stratagene) with the specific 5′-phosphorylated primers and were confirmed by sequencing.

Oocyte Water Permeability—The osmotic water permeability measurements were performed 3 days after injection of the cRNA. The oocyte-swelling assay was used for osmotic water permeability measurement. Oocytes were transferred into MBS diluted to 70 mosM with distilled water, and the time course of volume increase was monitored at room temperature by video microscopy with an online computer (6, 16). The relative volume (V/V_0) was calculated from the area at the initial time (A_0) and after a time interval (A_t): $V/V_0 = (A_t/A_0)^{3/2}$. The coefficient of osmotic water permeability (P_f) was determined from the initial slope of the time course ($d(V/V_0)/dt$), initial oocyte volume ($V_0 = 9 \times 10^{-4}$ cm^3), initial oocyte surface area ($S = 0.045$ cm^2), and the molar volume of water ($V_w = 18$ cm^3/mol) as shown in Equation 1.

$$P_f = (V_0 \times d(V/V_0)/dt)/(S \times V_w \times (osM_{in} - osM_{out})) \quad \text{(Eq. 1)}$$

Single-channel Recordings—The electrophysiological measurements were performed 1 day after injection of the cRNA. On the day of recording, oocytes were placed in a hypertonic solution (200 mM potassium aspartate, 20 mM KCl, 1 mM $MgCl_2$, 10 mM EGTA, 10 mM HEPES, pH 7.2 with KOH) for 10–15 min to facilitate manual removal of the vitelline membrane, and then the oocytes were placed in OR2 solution until use. Recordings were performed using both cell-attached and outside-out excised patch configurations. Patch pipettes made of borosilicate glass (World Precision Instruments) filled with the standard solution (see below) with resistances of 5–8 MΩ were used. The bath was grounded via a 3 M KCl-agar bridge connected to a Ag-AgCl reference electrode. Solution changes were performed by gravity-feed of the 300-μl chamber (Warner Instruments) at a speed of 10 ml/min. Data were acquired with an Axopatch 200A amplifier controlled by Clampex 7.0 (Axon Instruments) via a Digidata 1200 interface. Data were analyzed by Pclamp software.

Solutions—The bath solution for cell-attached recording contained 100 mM NaCl, 10 mM HEPES (pH7.2), and 1 mM $MgCl_2$. The pipette solution for cell-attached recording contained 100 mM CsCl, 10 mM HEPES (pH 7.2), 2 mM $MgCl_2$, and 5 mM EGTA, with or without 30 μM $HgCl_2$. The bath solution for outside-out recording contained 100 mM NaCl, 10 mM HEPES (pH 7.2), 1 mM $MgCl_2$, pH 7.2, with or without 10 μM $HgCl_2$. To substitute gluconate for chloride, 100 mM NaCl was replaced with 100 mM sodium gluconate. The one-third NaCl solution contained 33 mM NaCl, 10 mM HEPES (pH 7.2), 1 mM $MgCl_2$, and 132 mM mannitol. The pipette solution for outside-out recording contained 100 mM NaCl, 10 mM HEPES, 2 mM $MgCl_2$, 5 mM EGTA, pH 7.2.

Two-electrode Voltage Clamp—Whole oocyte membrane currents were recorded by a two-electrode voltage clamp. The standard isoosmotic solution contains 100 mM NaCl, 2 mM KCl, 1 mM $MgCl_2$, and 5 mM HEPES (pH 7.5). The command voltage was applied by two-microelectrode voltage clamp amplifier (Axoclamp-2A, Axon instruments, Foster City, CA) controlled by an IBM-compatible computer running pCLAMP software (Axon instruments, Foster City, CA). Current signals were sampled at 100 μs. The membrane potential was held at $V_{hold} = -50$ mV. To obtain current-voltage relationships, the membrane potential was rapidly stepped from the holding potential to a series of values generated between +50 and −150 mV, each differing by 20 mV. The pulse duration is 100 ms, and currents from 10 runs were averaged to reduce noise. All measurements were done at room temperature. Healthy oocytes were selected with resting potentials (from −25 to −40 mV).

Analysis of Hg^{2+} Activation Based on the Hill Equation—Hg^{2+}-induced membrane conductance of AQP6 oocytes was measured in OR2 solution containing the indicated concentrations of $HgCl_2$. The conductance was fitted to the Hill equation, and the Hill coefficient was calculated as shown in Equation 2,

$$G = G_{max}[Hg^{2+}]^n/(K_{0.5}{}^n + [Hg^{2+}]^n) \quad \text{(Eq. 2)}$$

where G_{max} is the maximum conductance at saturating external Hg^{2+} concentration, $K_{0.5}$ is the concentration of Hg^{2+} where the conductance is one-half of the maximum and n is the Hill coefficient.

$^{22}Na^+$ Influx Measurements—Oocytes were placed in Eppendorf vials and washed twice with OR2 solution. At the beginning of the experiment each vial received ^{22}NaCl (10 μCi, Amersham Biosciences) (17). After 90 s of incubation at room temperature, the oocytes were washed with ice-cold isotope-free OR2 solution. Each oocyte was immediately placed individually in a scintillation counter after addition of 5 ml of scintillation fluid.

Computer Modeling of Aquaporin-6 Structure—A crystal structure of bovine aquaporin-1 produced by x-ray diffraction to 2.2 Å (PDB coordinates: 1J4N) (8) was used as the template. Tetrameric coordinates were built by the European Bioinformatics Institute (EBI) Protein Quaternary Structure (PQS) server. The amino acid sequence of rat aquaporin-6 was threaded through the quaternary structure template in Swiss PDB Viewer 3.7 (b2) then optimized by the Swiss Institute of Bioinformatics (SIB) SWISS-MODEL automated protein modeling server.

RESULTS

We previously demonstrated that Hg^{2+} activates AQP6, increasing both the osmotic water permeability and the ion conductance 8–10-fold over baseline (4). The ion permeation through AQP6 allows us to study the single-channel electrophysiological behavior of AQP6. To determine whether AQP6 is gated, single-channel activity was recorded in cell-attached patches from plasma membranes of oocytes expressing rat AQP6 and compared with control oocytes injected with water (Fig. 1). The membrane potential was estimated as the inverse of the holding potential because the resting membrane

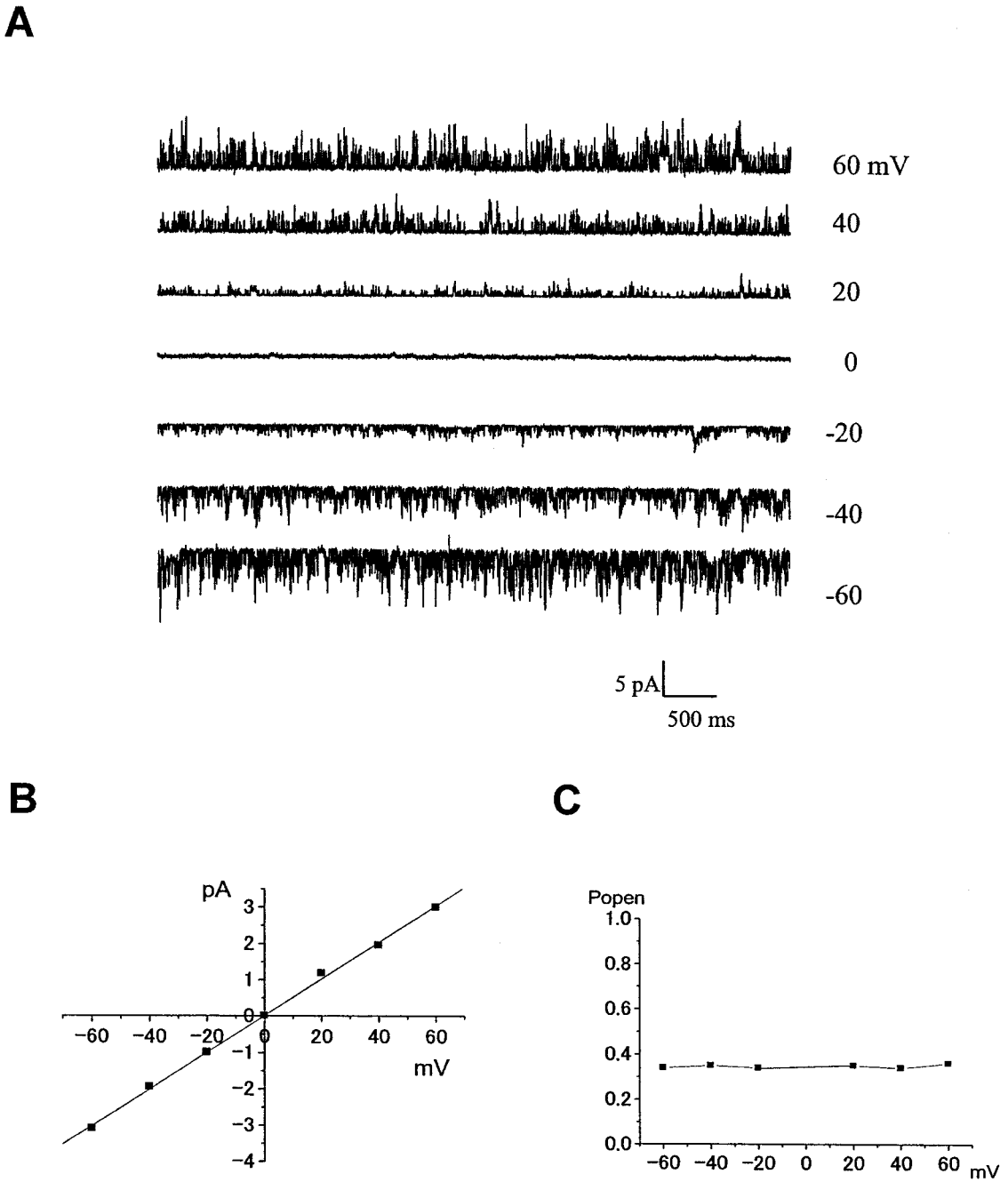

FIG. 2. **I-V relationship of the Hg^{2+}-induced single-channel currents.** *A*, representative single-channel currents are shown at different membrane potentials in a cell-attached recording. Although the resting membrane potential is usually uncertain in a cell-attached recording, the resting membrane potential in the present study was considered to be zero because of the manual removal of the vitelline membrane. Under these conditions, the membrane potential is considered to be the reverse of the pipette potential. *B*, I-V curve of 30 μM Hg^{2+}-induced AQP6 single-channel activities. (Shown are the means from three independent experiments.) *C*, open probability of AQP6 single-channel currents at different membrane potentials in the cell-attached recording. (Shown are the means from three independent experiments.)

potential of oocytes became almost zero during removal of the vitelline membrane. A time-dependent increase in AQP6 single-channel activity was observed after the application of 30 μM $HgCl_2$ into the patch pipette, whereas no increased channel activity was seen in recordings of plasma membranes of oocytes injected with water. Attempts to study single-channel conductance induced below pH 4.0 were prevented by difficulties in holding the patch pipette because of acidic conditions.

A linear I-V relationship was observed in cell-attached recordings of Hg^{2+}-induced single-channel currents in oocyte membranes expressing AQP6 (Fig. 2). The unitary conductance for the Hg^{2+}-activated channel in the cell-attached recording was 49 picosiemens, which was calculated from the slope conductance. The open probability of single-channel currents did not show any voltage dependence, suggesting that Hg^{2+}-activated AQP6 is not a voltage-gated channel.

To elucidate if the rapid induction of AQP6 by $HgCl_2$ is due to an increase in open probability of the channel, single-channel activity in an excised outside-out patch from the AQP6-expressing oocyte was recorded. Application of 10 μM $HgCl_2$ to the bath increased the open probability within 10 s (Fig. 3). Bath application of 0.5 mM β-mercaptoethanol reversed the effects of $HgCl_2$ only when it was applied within 1 min after

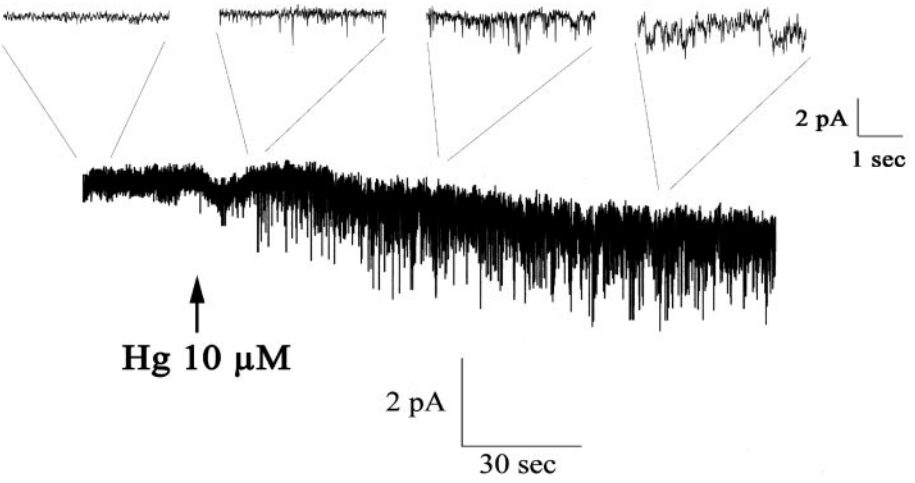

FIG. 3. **Outside-out recording.** Continuous recording of membrane currents of AQP6-expressing oocyte in an excised out-side out patch mode. 10 μM $HgCl_2$ was added to the bath solution (indicated by an *arrow*). Current traces with expanded time scale at several time points are also shown (n = 4).

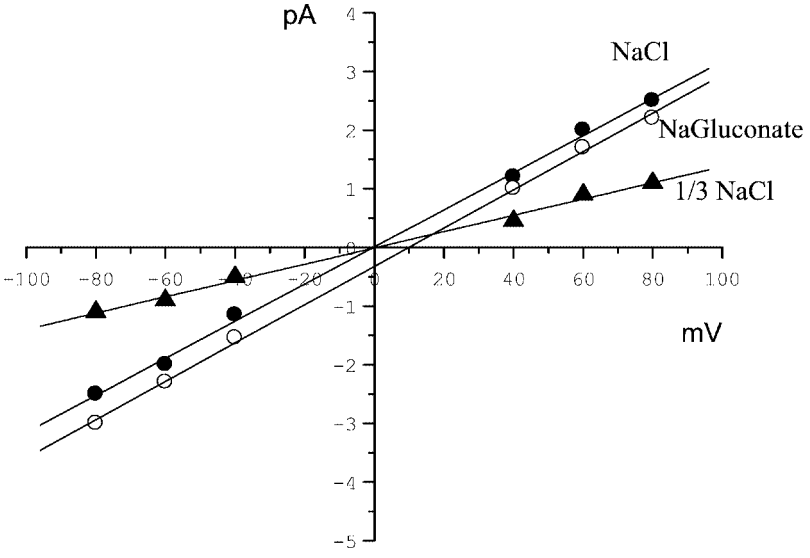

FIG. 4. **Ion selectivity of Hg^{2+}-induced single-channel currents.** Representative I-V curves obtained from outside-out recording of an AQP6-expressing oocyte in 100 mM NaCl (*closed circle*), 100 mM sodium gluconate (*open circle*), or 33 mM NaCl (*closed triangle*) (n = 3).

$HgCl_2$ application (not shown).

We previously showed that AQP6 exhibited anion selectivity when it was activated by low pH. To examine the ion selectivity of AQP6 induced by $HgCl_2$, ion replacement was performed in the excised outside-out patch mode. Ion replacement of chloride by gluconate shifted the reversal potential by +9.7 mV. Reduction of both Na^+ and Cl^- concentrations from 100 to 30 mM did not shift the reversal potential, indicating that both Na^+ and Cl^- are equally permeable (Fig. 4). This is clearly different from the ion selectivity of low pH-inducible AQP6, which was five times more permeable for Cl^- than Na^+ (4). To confirm Hg^{2+}-induced cation permeability, $^{22}Na^+$ influx was measured in AQP6-expressing oocytes or water-injected oocytes (control). In the absence of $HgCl_2$, $^{22}Na^+$ uptake was nearly equal for AQP6 and control oocytes (Fig. 5). The addition of 100 μM $HgCl_2$ to the bath solution caused a 2.6-fold increase of $^{22}Na^+$ uptake in AQP6 oocytes (from 11.0 ± 1.2 to 28.3 ± 5.3 cpm/oocyte/90 s, n = 5) but only a marginal increase in water-injected control oocytes (from 8.8 ± 1.4 to 12.0 ± 2.5 cpm/oocyte/90 s, n = 5), indicating that $HgCl_2$ induced Na^+ permeability of AQP6 oocytes consistent with the electrophysiological findings (Figs. 4 and 5).

Mercurials inhibit the water permeability of most aquaporins including AQP1 for which Cys-189 was identified as the single site of mercurial inhibition. To identify the residues responsible for Hg^{2+} activation of AQP6, site-directed mutagenesis was performed. Three cysteines are present in rat AQP6: Cys-6, Cys-155, and Cys-190. The C6S mutant exhibited Hg^{2+}-inducible water permeability and ion conductance similar to those of wild-type AQP6 (Fig. 6). C155A and C190A each exhibited less Hg^{2+}-inducible water permeability and ion conductance than did wild-type AQP6. The double mutant C155A/C190A exhibited negligible Hg^{2+}-activation. Dose-dependent effects of $HgCl_2$ on the conductance of AQP6-expressing oocyte was fitted to the Hill equation (Fig. 7). The Hill coefficient was 1.11 ± 0.28. Thus, Hg^{2+} binds to either the Cys-155 or the Cys-190 in each monomer to activate AQP6.

DISCUSSION

The aim of this study was to characterize the single-channel properties of AQP6 and to characterize the molecular mechanisms by which Hg^{2+} activates AQP6. We previously showed the ionic permeation of AQP6-expressing oocytes using a two-electrode voltage clamp (4). Here we used a single-channel patch clamp approach to examine the single-channel behavior of AQP6. Cell-attached patch recordings indicated that AQP6 is a gated channel induced by $HgCl_2$ in a time-dependent manner. The I-V relationship from single-channel recordings indicated no voltage dependence, consistent with our previous findings obtained from a two-electrode voltage clamp (4). The excised outside-out patch recording revealed a rapid activation of AQP6 by $HgCl_2$, which is reversed rapidly by the application of β-mercaptoethanol. We have demonstrated that AQP6 activation is achieved by Hg^{2+} binding to

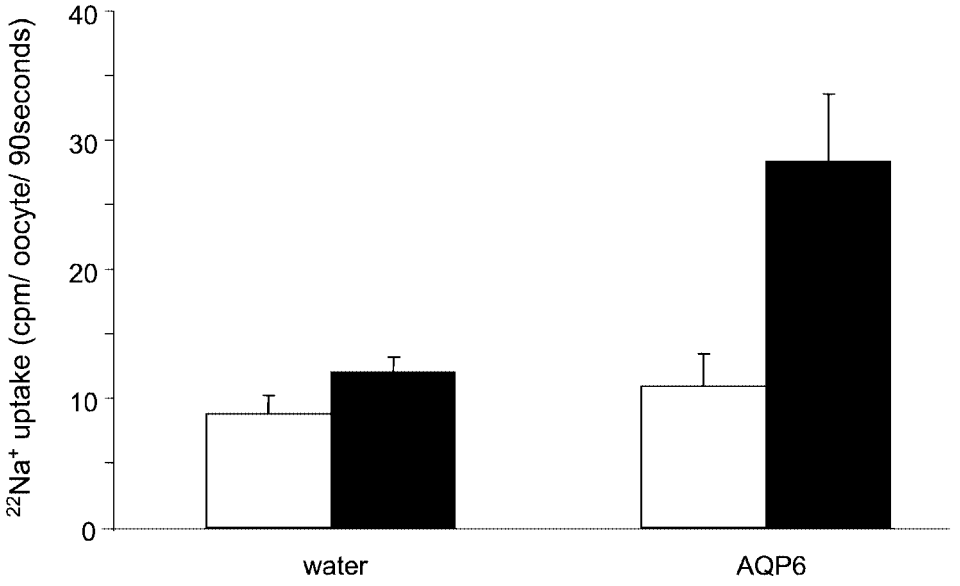

FIG. 5. **Radio-isotope influx measurements with $^{22}Na^{+}$.** AQP6-expressing oocytes or water-injected oocytes (control) were incubated for 90 s in OR2 containing 10 μCi of $^{22}Na^{+}$. $^{22}Na^{+}$ uptake was measured in the absence (*open bars*) or presence of 100 μM $HgCl_2$ (*closed bars*). Shown is the mean ± S.E., $n = 5$.

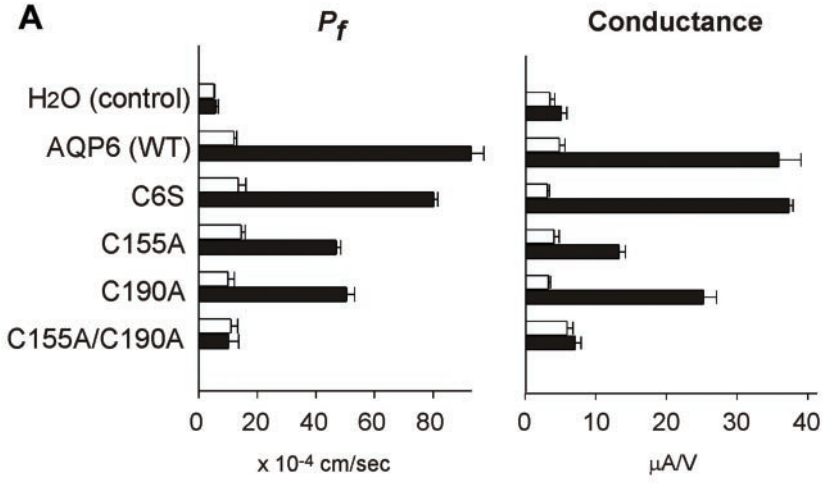

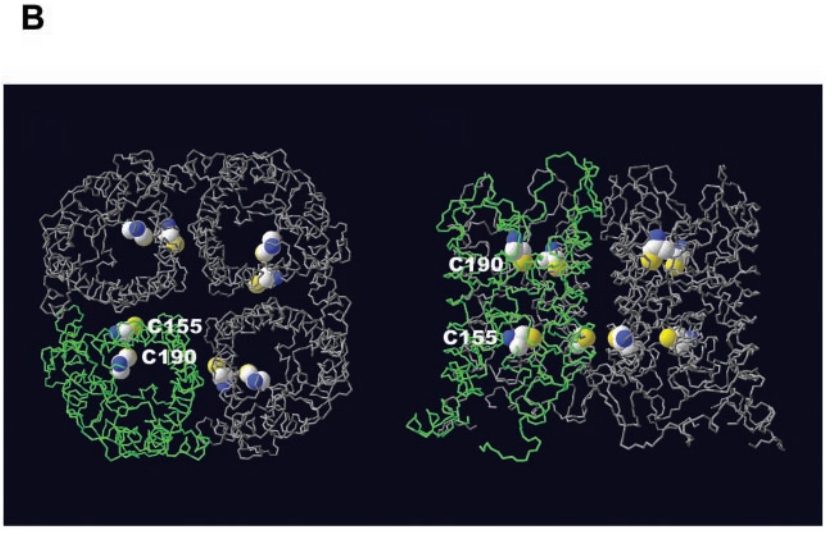

FIG. 6. **$HgCl_2$ activation of water permeability and ion conductance of AQP6 oocyte.** *A*, oocytes were injected with 5 ng of the indicated cRNA or 50 nl of water for control. The coefficients of osmotic water permeability were assessed by the swelling assay 3 days after injection with or without 300 μM $HgCl_2$ (*left panel*). The ion conductance was determined by two-electrode voltage clamp 2 days after injection with or without 100 μM $HgCl_2$ (*right panel*). Shown is the mean ± S.E., $n = 5$. *B*, the peptide backbone of computer-modeled tetrameric rat aquaporin-6 is depicted from the extracellular face (*left*) and from the side (*right*). One monomer is colored *green* for clarity. Cysteine residues 155 and 190 are *highlighted* by van der Waals space-filling; the sulfhydryl groups are *yellow*. The figure was produced with Swiss PDB Viewer.

Cys-155 or Cys-190 residue in each monomer. Site-directed mutagenesis revealed that changes in water permeability resulted in equivalent changes in ion conductance. Taken together, these data suggest that each monomer forms a pore region for water and ions rather than ionic permeation through the center of homotetramer.

Aquaporins are homotetramers with each monomer providing an independent water pore. In contrast, the conducting

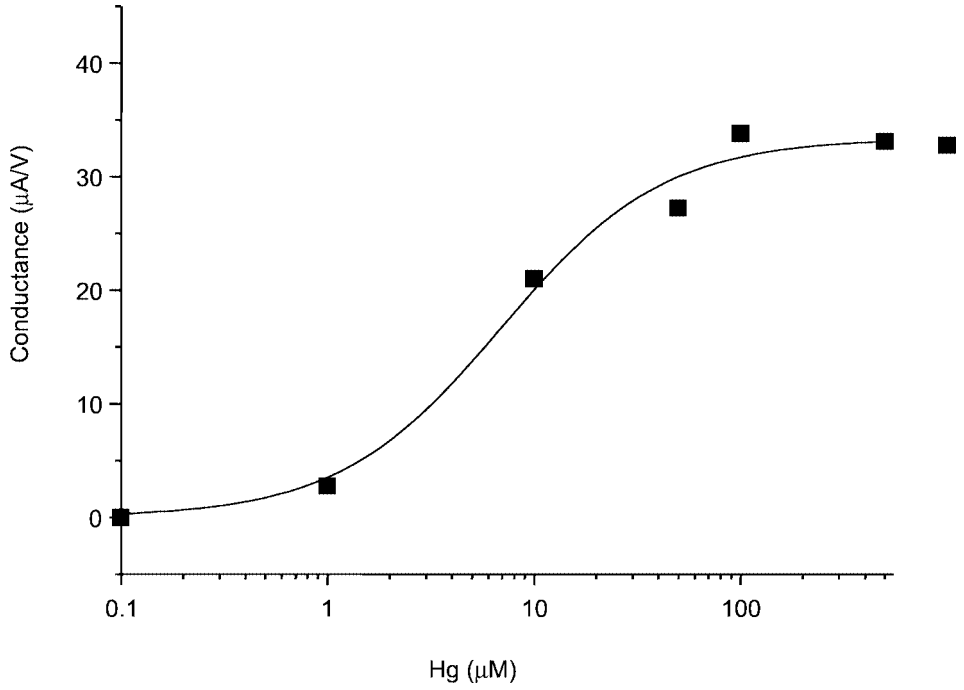

FIG. 7. **Dose-dependent conductance of an AQP6 oocyte treated with $HgCl_2$.** The average membrane conductance of an AQP6-expressing oocyte is shown as fitted to the Hill equation (n = 3–5). The conductance was calculated from the slope of the I-V curve between +10 and −90 mV obtained 1 min after application of the indicated concentration of $HgCl_2$ by a two-electrode voltage clamp. All values in fitting are the calculated parameter ± S.D.

multimeric pore in many ion channels exists at the central 4-fold axis of symmetry. The 4-fold symmetry axis of GlpF has been considered as a potential pathway for ions because the dimensions along the axis are similar to those of the tetrameric KcsA potassium channel (15). We do not have direct evidence to conclude whether this is the case for AQP6; however, we strongly suspect that the each monomer contains an ion pore. We have found that each monomer has two Hg^{2+} binding sites, Cys-155 and Cys-190, indicating that there are eight Hg^{2+} binding sites in the homotetramer. Nevertheless, the Hill coefficient for Hg^{2+} binding is nearly unity, indicating no allosteric effects. Therefore, it is not likely that the 4-fold symmetry axis of AQP6 is the pore for ions. Structural analysis of AQP6 should identify the definitive ionic pathway for AQP6; however, attempts to express and purify the protein have so far been unsuccessful.

Our studies with AQP6 contrast markedly with studies of AQP1 that purportedly led a subset of investigators to conclude that AQP1 functions as an ion channel. Previously reports (18) have shown that oocytes expressing AQP1 contain forskolin-induced membrane currents, although we and other investigators could not confirm this (2). Subsequently, it was reported that stimulation with high concentrations of cGMP activated membrane currents in AQP1 oocytes (19). This observation was qualitatively confirmed in planar bilayers containing purified AQP1; however, the cGMP-induced currents were activated very slowly, and, curiously, less than one in 10^6 AQP1 water channels was permeated by ions (3). Although the biological significance (or lack of significance) of AQP1 ion conductance is debated, it is agreed that the AQP1 water and ion pathways are not identical. Thus, it is likely that the exceedingly rare currents through AQP1 probably represent slippage through the 4-fold axis and do not resemble ion conductance through the aqueous pore in each subunit of AQP6.

Mercurials are known as inhibitors of aquaporins (5). An earlier report of AQP6 showed inhibition of water permeability by $HgCl_2$ (10). Surprisingly, we showed that $HgCl_2$ activates AQP6 (4). It is intriguing that the binding of Hg^{2+} to the corresponding sites (Cys-189 for AQP1 and Cys-190 for AQP6) leads to inhibition of AQP1 but activation of AQP6. We demonstrated that the binding of Hg^{2+} to AQP6 increased open probability of the channel gating. At this point, we could not distinguish whether the binding of Hg^{2+} to AQP1 simply occludes the pore or decreases the open probability of the channel because there is no evidence of rapid channel gating for AQP1. Cys-155 is the other binding site for Hg^{2+} to activate AQP6. The corresponding residue for Cys-155 is Cys-152 for AQP1 (6); however, Hg^{2+} has no effect on Cys-152 in AQP1. This also suggests that the mechanisms of Hg^{2+} effect on AQP6 are different from those of AQP1.

We previously showed that low pH-induced AQP6 current is anion selective, based on reversal potentials measured in ion substitution experiments (4). In contrast, Hg^{2+}-induced AQP6 current exhibits much less ion selectivity. We hypothesize that pharmacological activation of AQP6 with Hg^{2+} leaves the pore in the maximally open state, which is probably not achieved physiologically. Nevertheless, the Hg^{2+}-activation studies provide a new approach for molecular dissection of an ion channel. We believe that activation by low pH represents a physiologically open state that can be driven rapidly. The induction of water permeability of AQP6 by low pH is limited compared with the Hg^{2+}-induced water permeability (4). This may support our hypothesis that the pore open state is different between low pH-induced and Hg^{2+}-induced AQP6 and that the characteristic of AQP6 as an anion channel is physiologically more relevant. Hg^{2+} activation and ionic permeation are unique characteristics of AQP6, as is gating. We believe that biophysical analysis of AQP6 will provide fundamental and novel insights into new functions of aquaporins and will form the basis for subsequent examination of structure-function relationships of the aquaporin channel family.

Acknowledgment—We thank Masahiro Ikeda for a helpful discussion and critical reading of the manuscript.

REFERENCES

1. Agre, P. (2000) *J. Am. Soc. Nephrol.* **11,** 764–777
2. Agre, P., Lee, M. D., Devidas, S., and Guggino, W. B. (1997) *Science* **275,** 1490
3. Saparov, S. M., Kozono, D., Rothe, U., Agre, P., and Pohl, P. (2001) *J. Biol. Chem.* **276,** 31515–31520
4. Yasui, M., Hazama, A., Kwon, T. H., Nielsen, S., Guggino, W. B., and Agre, P. (1999) *Nature* **402,** 184–187
5. Macey, R. I. (1984) *Am. J. Physiol.* **246,** C195-C203
6. Preston, G. M., Jung, J. S., Guggino, W. B., and Agre, P. (1993) *J. Biol. Chem.* **268,** 17–20
7. Murata, K., Mitsuoka, K., Hirai, T., Walz, T., Agre, P., Heymann, J. B., Engel, A., and Fujiyoshi, Y. (2000) *Nature* **407,** 599–605
8. Sui, H., Han, B. G., Lee, J. K., Walian, P., and Jap, B. K. (2001) *Nature* **414,** 872–878
9. de Groot, B. L., and Grubmuller, H. (2001) *Science* **294,** 2353–2357
10. Ma, T., Yang, B., Kuo, W. L., and Verkman, A. S. (1996) *Genomics* **35,** 543–550
11. Smith, B. L., and Agre, P. (1991) *J. Biol. Chem.* **266,** 6407–6415
12. Verbavatz, J. M., Brown, D., Sabolic, I., Valenti, G., Ausiello, D. A., Van Hoek, A. N., Ma, T., and Verkman, A. S. (1993) *J. Cell Biol.* **123,** 605–618
13. Mitra, A. K., Yeager, M., Van Hoek, A. N., Wiener, M. C., and Verkman, A. S. (1994) *Biochemistry* **33,** 12735–12740
14. Walz, T., Smith, B. L., Agre, P., and Engel, A. (1994) *EMBO J.* **13,** 2985–2993
15. Fu, D., Libson, A., Miercke, L. J., Weitzman, C., Nollert, P., Krucinski, J., and Stroud, R. M. (2000) *Science* **290,** 481–486
16. Preston, G. M., Carroll, T. P., Guggino, W. B., and Agre, P. (1992) *Science* **256,** 385–387
17. Weber, W. M., Liebold, K. M., and Clauss, W. (1995) *Biochim. Biophys. Acta* **1239,** 201–206
18. Yool, A. J., Stamer, W. D., and Regan, J. W. (1996) *Science* **273,** 1216–1218
19. Anthony, T. L., Brooks, H. L., Boassa, D., Leonov, S., Yanochko, G. M., Regan, J. W., and Yool, A. J. (2000) *Mol. Pharmacol.* **57,** 576–588 .0